Applied Catalysis B: Environmental 142–143 (2013) 178–186

Contents lists available at SciVerse ScienceDirect

Applied Catalysis B: Environmental

journal homepage: www.elsevier.com/locate/apcatb

On the structure and hydrotreating performance of carbon-supported CoMo- and NiMo-sulfides

A.I. Dugulan [a], J.A.R. van Veen [b,c], E.J.M. Hensen [b,*]

[a] Reactor Institute Delft, Delft University of Technology, Mekelweg 15, 2629 JB, Delft, The Netherlands
[b] Schuit Institute of Catalysis, Eindhoven University of Technology, P.O. Box 513, 5600 MB, Eindhoven, The Netherlands
[c] Shell Global Solutions International B.V., P.O. Box 38000, 1030 BN, Amsterdam, The Netherlands

ARTICLE INFO

Article history:
Received 2 March 2013
Received in revised form 2 May 2013
Accepted 8 May 2013
Available online 15 May 2013

Keywords:
Hydrotreating
Carbon support
'Co–Mo–S'
HDS
HDN

ABSTRACT

The sulfiding behaviour and hydrotreating performance of CoMo and NiMo on carbon catalysts were investigated, with a view to establishing the suitability of an active-carbon carrier for industrial hydrotreatment purposes. The sulfidation process (H_2/H_2S at 0.1 and 4 MPa) was followed with ^{57}Co Mössbauer emission spectroscopy, and X-ray absorption spectroscopy (Mo- and Co-edge). It turns out that the structural evolution of the CoMo/C catalyst is in broad terms very similar to that of a $CoMo/Al_2O_3$ one, including the type I → II phase transition at increased sulfiding pressure, albeit that some sintering takes place concomitantly. In the hydrotreating part a NiMo/C catalyst was employed, sulfided at 1 or 4 MPa, in trickle-flow conditions at 3.5 (HDS) and 6 (HDN) MPa. It transpires that the adsorption properties of NiMo/C are quite different from those of a NiMo/alumina, in that dibenzthiophene, quinoline, and polyaromatics are much stronger adsorbed on the carbon-supported catalyst. This leads to very high dibenzothiophene HDS and quinoline HDN activities, but to a disappointing performance in the hydrotreatment of a heavy gasoil, where the polyaromatics can compete effectively for adsorption on the active HDS/N sites.

1. Introduction

The removal of organic sulfur and nitrogen compounds from crude oil feedstock continues to be one of the pivotal processes in oil refineries to arrive at clean transportation fuels that meet ever-tightening environmental legislation. Hydrodesulfurization (HDS) and hydrodenitrogenation (HDN) catalysts typically consist of mixed metal sulfides of Co or Ni and Mo dispersed on γ-alumina. There is by now overwhelming evidence that the active phase consists of atomically dispersed Co or Ni sulfide on the edges of MoS_2 slabs ('Co–Mo–S' phase) [1–5]. ^{57}Co Mössbauer emission spectroscopy (MES) is usually employed to interrogate the sulfided catalyst about the presence of Co in the 'Co–Mo–S' phase and in other less active phases such as bulk Co sulfides and Co-aluminates [6–8]. ^{57}Co MES and EXAFS studies revealed that at higher Co/Mo atomic ratios the Co sulfide species at the edges of the MoS_2 slabs can differ in size and/or ordering [9,10]. It is well known that the support can have a strong influence on the hydrotreating performance of such mixed sulfide phases. The most important support-related issues for hydrotreating catalysts have been recently reviewed by Breysse et al. [11]. A systematic study on the performance of 'Co–Mo–S' phases in thiophene HDS was carried out by van Veen et al. [12]. For alumina-supported catalysts two types of Co–Mo–S structures were proposed [13]: an incompletely sulfided type I phase with some residual linkages to the alumina support and a more active type II Co–Mo–S, where all such Mo–O–Al linkages are completely sulfided. The formation of the latter phase can also be induced by the use of complexing agents [12]. Although γ-alumina is the preferred support for industrial hydrotreating catalysts, it is known that the use of activated carbon carriers can result in very active HDS catalysts [12,14–16]. The high activity of carbon-supported M′Mo-sulfides (M′ = Co or Ni) in thiophene HDS is believed to originate from the weak interaction of the active sulfide phase with the support, resulting in the exclusive presence of type II 'Co–Mo–S' structures [12,17]. Such catalysts also show benefit in gas-phase HDS reactions of DBT and substituted DBTs [18]. Type II 'M′–Mo–S' supported on activated carbon is about twice as active as when it is supported on γ-alumina. It is also worthwhile to mention that carbon-supported Co-sulfide catalysts can display very high activity in thiophene HDS [14,19–23].

Sulfidation in nearly all of these studies was done in H_2S/H_2 mixtures at atmospheric pressure, which considerably deviates from commercial practice. An early MES study of the effect of high-pressure sulfidation on alumina-supported CoMo suggested

* Corresponding author. Tel.: +31 40 2475178.
E-mail address: e.j.m.hensen@tue.nl (E.J.M. Hensen).

0926-3373/$ – see front matter © 2013 Elsevier B.V. All rights reserved.
http://dx.doi.org/10.1016/j.apcatb.2013.05.013

that the 'Co–Mo–S' phase might dissociate [13]. Dugulan et al. recently investigated the effect of sulfidation on a CoMo/C catalyst [24]. The most important conclusions of that study were that (i) high-pressure sulfidation of CoMo/C resembles that of CoMo/γ-Al_2O_3 and is different from atmospheric-pressure sulfidation of CoMo/C (which gives rise to highly dispersed Co-sulfide) and (ii) CoS_x segregates from the 'Co–Mo–S' phase at lower temperature than observed in the case of an γ-alumina support. The segregation in this particular study may however have been caused by the Co content of the CoMo/C catalyst (atomic Co/Mo ratio = 0.52), which is typically regarded as too high to render a stable 'Co–Mo–S' phase at typical MoS_2 dispersions.

In view of the potential of carbon-supported M′Mo sulfides in model studies, we expand on the above issues with the aim to explore the stability of 'M′–Mo′–S' phases in carbon-supported hydrotreating catalysts and evaluate their performance in more realistic trickle-flow test reactions. Breysse et al. have stressed the importance of carrying out real gas oil hydrotreating tests for catalysts with improved performance in model reactions [11]. Kouzu et al. showed the potential of a carbon-supported NiMo sulfide catalysts for ultradeep HDS [25], while Prabhu et al. reported improved performance in light gas oil hydrotreating by a NiMo catalyst supported on a mesoporous carbon [26]. Herein, to evaluate active phase stability we will employ a CoMo/C catalyst with an optimal Co/Mo ratio of 0.3 and compare its ^{57}Co MES spectra obtained under high-pressure sulfidation conditions to earlier data for CoMo/C [24] and CoMo/γ-Al_2O_3 [27,28]. The evolution of catalyst structure during sulfidation is followed by Co and Mo EXAFS. The performance of these catalysts is first compared in gas-phase dibenzothiophene (DBT) HDS. Then, after finding that high-pressure sulfidation even further improves the gas-phase DBT HDS activity of the carbon-supported catalyst, we studied the performance of a carbon-supported M′Mo catalyst under more realistic conditions: that is, we evaluated the performance of a NiMo/C catalyst against an alumina-supported analogue in trickle-flow mode, first in single-component DBT HDS and quinoline HDN reactions, in view of the known differences in catalyst rankings in gas- vs. liquid-phase mode [29], and then in the hydrotreating of an industrial heavy gas oil feed.

2. Experimental

CoMo catalysts were prepared by pore-volume impregnation using activated carbon (Norit RX3-extra, BET surface area 1197 $m^2\,g^{-1}$, pore volume 1.0 $ml\,g^{-1}$, particle size 0.5–0.85 mm) as support material. Aqueous solutions of cobalt nitrate $Co(NO_3)_2{\cdot}6H_2O$ (Merck p.a.) and ammonium heptamolybdate $(NH_4)_6Mo_7O_{24}{\cdot}4H_2O$ (Merck, min. 99.9%) were used in a two-step impregnation procedure. Molybdenum was first introduced and the catalysts were dried in static air at 110 °C for 16 h. About 50 MBq ^{57}Co as an aqueous solution of $Co(NO_3)_2{\cdot}6H_2O$ was added to the Co-containing impregnation solution. After introduction of cobalt, the catalyst was left in static air at room temperature for 16 h. The catalysts contained 7 wt% Mo. One catalyst was prepared at a Co loading of 2.25 wt% (Co(2.25)Mo(7)/C, atomic Co/Mo ratio of 0.52), one at 1.3 wt% (Co(1.3)Mo(7)/C, atomic Co/Mo ratio of 0.3) and one at 0.04 wt% ((Co(0.04)Mo(7)/C, atomic Co/Mo ratio of 0.009). The catalyst loadings are given relative to the support material and are calculated from the impregnation solutions. Samples were sulfided in a flow of 60 N mL min^{-1} of 10% H_2S/H_2 mixture in a high-pressure Mössbauer in situ reactor. The sulfidation treatment is denoted by the postfix (S, *x* MPa, *y* K, *z* h), indicating that the catalyst is linearly heated to *y* K at *x* MPa in 1 h and kept at this temperature for *z* h. For comparison, a CoMo/γ-Al_2O_3 catalyst was prepared by co-impregnation of Ketjen CK-300 with a solution containing appropriate amounts of $Co(NO_3)_2{\cdot}6H_2O$, $(NH_4)_6Mo_7O_{24}{\cdot}4H_2O$ and nitrilotriacetic acid (NTA) (7 wt.% Mo, 2.25 wt% Co and a molar NTA/Mo ratio of 1.2) [12].

The ^{57}Co MES spectra were recorded at room temperature and at the sulfiding pressure. The setup for Mössbauer measurements was a constant acceleration spectrometer operated in triangular mode with a moving single-line $K_4Fe(CN)_6{\cdot}3H_2O$ absorber enriched in ^{57}Fe. The velocity scale was calibrated with a ^{57}Co:Rh source and a sodium nitroprusside (SNP) absorber. Zero velocity corresponds to the peak position of the $K_4Fe(CN)_6{\cdot}3H_2O$ absorber measured with the ^{57}Co: Rh source. Positive velocities correspond to the absorber moving towards the source. The spectra were analyzed with a Lorentzian fitting procedure [30].

The EXAFS spectra, measured at the Co K-edge (7.709 keV) and the Mo K-edge (20 keV), were obtained at the Dutch-Belgian Beamline (DUBBLE) at the European Synchrotron Radiation Facility (ESRF), Grenoble, France. The electron energy and ring current were 6 GeV and 150–200 mA, respectively. The catalysts were stepwise sulfided in stainless-steel tubular reactors that were subsequently flushed with Ar and opened in a glove box. Self-supporting wafers of the sulfided catalysts were pressed in the glove box and brought in an environmental cell. The thickness of the wafer was chosen to give an absorbance (μx) of about 2.5 in the Mo K-edge region to ensure an optimal signal-to-noise ratio. Because of the low Co concentration in the catalyst, the absorbance for the Co K-edge measurements was about 3. Three scans of each sample were recorded in transmission mode. Full details of the data analysis and of the quality of the fits obtained can be found in ref. [31], Chapter 2 (Section 2.2). Gas-phase catalytic tests were performed in a stainless-steel reactor with a feed consisting of 1.0 wt.% DBT dissolved in *n*-decane. The H_2 pressure was set at 3 MPa, the gas rate at 625 $Nl_{H2}\,kg_{feed}^{-1}$ and the S content in the gas phase was 200 ppm. The catalyst bed consisted of 20 mg of the catalyst diluted in SiC (1:1 on a volume basis) of the same sieve fraction (125–250 μm). Prior to activity measurements, the catalyst was sulfided as outlined above. Typically, 8 h were allowed at each reaction condition to ensure catalyst stabilization. Products were analyzed by online gas chromatography (HP 5890, CP-Sil-5CB, FID). First-order kinetics (k_{HDS}) were assumed for the HDS of DBT.

For the microflow trickle-bed catalytic tests, a NiMo catalyst was prepared via the nitrilotriacetic acid (NTA) route [12] on crushed activated carbon extrudates (30–80 mesh, Norit RX-3 extra). The Ni and Mo content were 1.8 and 8.2 wt%. The catalyst was sulfided in a mixture of 5.2 wt% t-nonylpolysulfide (corresponding to 2 wt% S) in *n*-hexadecane fed at a liquid rate of 1.4 h^{-1} with a gas rate of 250 $Nl_{H_2}\,kg_{feed}^{-1}$ and a pressure of 4 MPa under heating of the catalyst bed from 40 to 280 °C at 20 °C/h, an isothermal dwell at 280 °C for 5 h followed by heating to 340 °C at the same rate and a final isothermal dwell of 16 h. The catalyst was first tested in DBT HDS at a hydrogen pressure of 3.5 MPa, a gas rate of 250 $Nl_{H_2}\,kg_{feed}^{-1}$, the feed being 4.8 wt% DBT in *n*-hexadecane, and subsequently in quinoline HDN at a pressure of 6.0 MPa, a gas rate of 250 $Nl_{H_2}\,kg_{feed}^{-1}$, the feed consisting of 1560 ppmw N as quinoline in *n*-hexadecane. The catalyst loading was 3 g.

The catalytic activity was also determined in the hydrotreating of a catalytically cracked heavy gas-oil (CCHGO) in a trickle-bed configuration. The catalyst intake was 6 g, which was diluted with an equivalent volume amount of 60–80 mesh SiC. Sulfidation was done in the gas phase at 1.0 MPa in a flow of 24 Nl/h 12 vol% H_2S in H_2 under heating to 370 °C at a rate of 75 °C/h followed by an isothermal dwell of 2 h. The test conditions were as follows: T = 343 °C, p = 6.0 MPa, WHSV of 2.3 $kg_{feed}\,kg^{-1}\,h^{-1}$ and a gas rate of 400 $Nl_{H2}\,kg_{feed}^{-1}$. The feed (density 20/4 = 1.0136 g ml^{-1}) contained 88.5 wt% C, 8.8 wt% H, 2.59 wt% S, 900 ppmw N and 0.48 wt% O. A standard NiMoP/alumina catalyst (3.0%w Ni, 13%w Mo, 2.2%w P) served as a reference.

3. Results and discussion

3.1. Structural effects

Fig. 1 shows the ^{57}Co MES spectra of Co(1.3)Mo(7)/C and Co(2.25)Mo(7)/C sulfided at atmospheric pressure followed by high-pressure (4.0 MPa) sulfidation at the final temperature of 400 °C. The corresponding fit parameters are presented in Tables 1 and 2. The spectra of the fresh catalyst contain a quadrupole doublet indicating a low-spin 2+ or a 3+ phase and a second contribution consistent with Co^{2+} in the high-spin state [32]. Sulfidation at room temperature brings about a second contribution with an isomer shift (IS) around 0.20 mm s^{-1} and quadrupole splitting (QS) around 1.20 mm s^{-1}, indicative of the formation of a Co-sulfide phase. As typically observed with increasing sulfidation temperature [31], the QS value first decreases up to an intermediate sulfidation temperature followed by a small increase when sulfidation is completed. The increase (decrease) in QS is generally interpreted in terms of a decrease (increase) in the particle size and/or ordering of the Co-sulfide species [22]. It has been postulated that this behaviour is indicative of the interaction between CoS_x and the Mo-oxide/sulfide phase [28]. Indeed, the increase in QS is usually observed at temperatures at which the MoS_2 crystallites are formed and can, accordingly, be understood in terms of redispersion of the Co-sulfide particles over the edges of the MoS_2. A similar redispersion model has been proposed for NiS_x particles in NiW catalysts [33]. After 0.1 MPa sulfidation of Co(1.3)Mo(7)/C, the doublet has an IS value of 0.21 mm s^{-1} and a QS value of 1.05 mm s^{-1}. These parameters are characteristic for the 'Co–Mo–S' phase. When this sample is subsequently sulfided at 400 °C and 4 MPa, the QS value decreases only slightly. This result clearly shows that no segregation of a Co_9S_8 phase occurs in a CoMo/C catalyst with an optimal Co/Mo ratio. The results for Co(2.25)Mo(7)/C are different. The minimum QS value during the temperature-programmed sulfidation is lower than for Co(1.3)Mo(7)/C pointing to more extensive clustering of the Co-sulfide phase, which is consistent with the higher Co/Mo ratio. At a temperature of 300 °C at which one expects MoS_2 formation to be nearly complete, the QS is 0.85 mm s^{-1}. In this case, the QS value does not increase anymore after 0.1 MPa sulfidation at 400 °C. The QS value is well below the typical values associated with the 'Co–Mo–S' phase and, instead, point to the presence of a CoS_x phase. When the sulfidation pressure is increased to 4.0 MPa, segregation of Co-sulfide occurs as a second doublet becomes apparent in the MES spectra with a QS of 0.29 mm s^{-1}, indicative of Co_9S_8. This phase makes up about 37% of the Co atoms. The other Co atoms remain closely associated with the MoS_2 phase as evident from the QS value of ~1.0 mm s^{-1}. This result shows that the CoS_x phase formed upon 0.1 MPa sulfidation at 400 °C was in close proximity to the MoS_2 phase. These findings for 0.1 MPa sulfidation of Co(2.25)Mo(7)/C are consistent with those reported for direct 4.0 MPa sulfidation of the same catalyst. Albeit that high-pressure sulfidation already led to Co_9S_8 segregation at 300 °C, the contribution of Co_9S_8 is very similar in both cases after the final sulfidation step at 400 °C and 4.0 MPa. Importantly, these results confirm our initial surmise that the main reason for segregation of CoS_x in Co(2.25)Mo(7)/C was its too high Co/Mo ratio. No CoS_x segregation is observed for a catalyst with a close to optimal (in terms of performance) Co/Mo ratio, even after high-pressure sulfidation.

The fit parameters of the k^3-weighted EXAFS functions at the Mo K edge for Co(1.3)Mo(7)/C catalyst as a function of the sulfidation temperature and pressure are collected in Table 3. The spectrum of the catalyst sulfided at 200 °C was fitted by a Mo-S contribution at 2.46 Å and a Mo-Mo contribution at 2.73 Å. The Mo-Mo distance is smaller than the typical Mo–Mo distance of 3.16 Å in MoS_2 [34] and indicates that sulfidation is not complete yet. The Mo-S coordination number is relatively low, which is most likely caused by

Table 1
MES parameters of Co(1.3)Mo(7)/C catalyst after different sulfidation treatments.

T_s (°C)	P (MPa)	IS (mm s^{-1})	QS (mm s^{-1})	Γ (mm s^{-1})	A (%)	IS (mm s^{-1})	QS (mm s^{-1})	Γ (mm s^{-1})	A (%)	IS (mm s^{-1})	QS (mm s^{-1})	Γ (mm s^{-1})	A (%)
		"Co-oxide"				"Co-sulfide"				"High-spin 2+"			
Fresh		0.29	0.84	0.81	84					1.02	1.82	0.59	16
RT	0.1					0.19	1.24	0.73	100				
100	0.1					0.20	1.23	0.70	100				
200	0.1					0.21	0.91	0.67	100				
300	0.1					0.21	0.98	0.73	100				
400	0.1					0.21	1.05	0.79	100				
400	4					0.21	0.97	0.80	100				

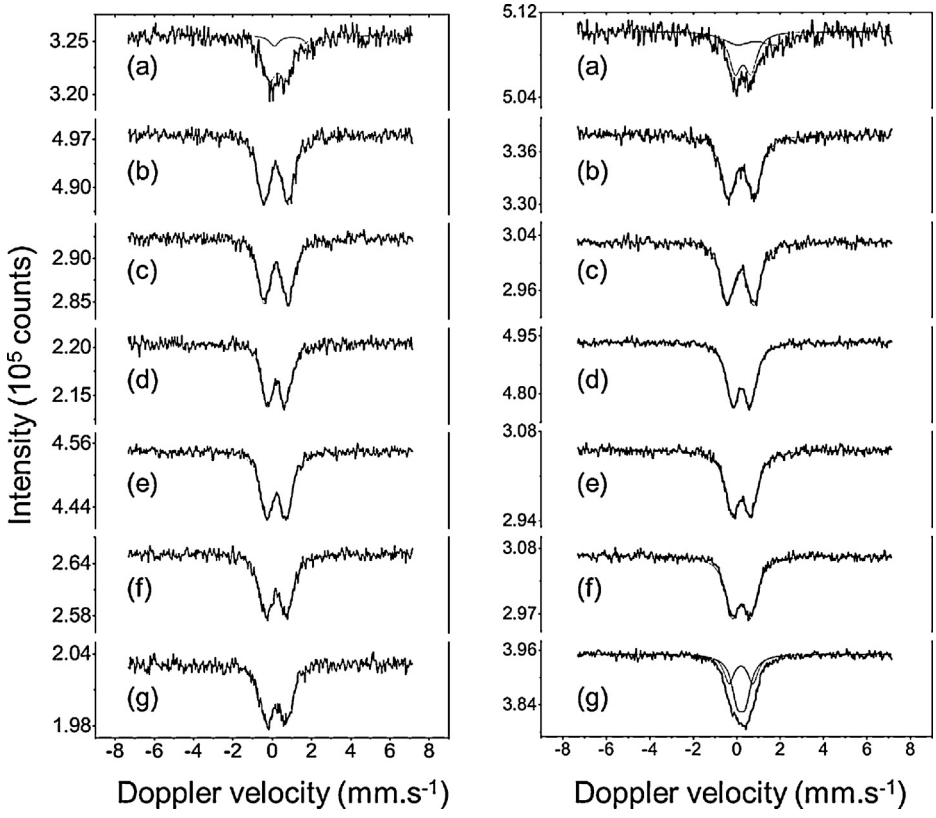

Fig. 1. Room temperature ^{57}Co Mössbauer emission spectra of (left) Co(1.3)Mo(7)/C and (right) Co(2.25)Mo(7)/C catalyst after various successive sulfidation steps: (a) fresh catalyst; (b) S, 0.1 MPa, 300 K; (c) S, 0.1 MPa, 373 K; (d) S, 0.1 MPa, 473 K; (e) S, 0.1 MPa, 573 K; (f) S, 0.1 MPa, 673 K and (g) S, 4 MPa, 673 K.

an overlap of Mo–O and Mo–S shells or an influence of the presence of Mo^{6+} [35,36]. After increasing the sulfidation temperature to 300 and 400 °C, the Mo–S and Mo–Mo interatomic distances are in agreement with the structural parameters of MoS_2 crystallites. A relatively low Mo-S coordination number (N_{Mo-S} = 5.3) is obtained after treatment at 400 °C and 0.1 MPa, indicating that the MoS_2 edges are not completely saturated with sulfur. Previous XPS and EXAFS studies have shown for carbon-supported catalysts Mo-S coordination numbers, structural order and stacking degree similar to Type I Co–Mo–S catalysts supported on alumina [37]. A relatively strong MoS_2-carbon support interaction or physical trapping of the MoS_2 particles in the micropores of the support were proposed. Why in the latter case the Mo–S coordination number should be low, however, is a moot point: perhaps we have both a strong support interaction and trapping in the micropores (see below). After increasing the sulfidation pressure to 4.0 MPa, the Mo–S coordination number of 5.3 increases to 5.7, which indicates the expected evolution towards a type II 'Co–Mo–S' phase, although the number remains a bit on the low side, so that the transformation is possibly not complete. The data also show that the Mo–Mo coordination number increases when the sulfidation degree is increased, which may be explained by increasing crystallinity/ordering of the MoS_2 phase or to some sintering. From these findings, we speculate that the interaction between the MoS_2 phase and the activated carbon carrier may be larger than one would anticipate. As the Mo–Mo coordination number after 4.0 MPa sulfidation is quite similar to what is typically reported for alumina-supported CoMo catalysts, we may safely assume that the MoS_2 dispersion in our carbon-supported CoMo case remains high. Finally, it is noteworthy that clearly distinguishable Mo–Co backscatterers appear in the Mo K-edge spectra after 4.0 MPa sulfidation, as they should for a well-defined Co–Mo–S phase, evidencing an increased ordering of the MoS_2 particles. The coordination distances for the interaction of the promoter with the MoS_2 slabs are in good agreement with previous reports [22,38].

The Co K-edge EXAFS results for Co(1.3)Mo(7)/C are shown in Table 4. After sulfidation at 200 °C and 0.1 MPa, the presence of Co–S (2.22 Å) and two Co–Co (2.56 and 3.29 Å) evidence that Co is already sulfided and that some clustering has occurred in line with the MES results. The Co–Co coordination distances are substantially different from those for bulk Co_9S_8 (2.51 Å and 3.51 Å). Together with the low coordination numbers for the Co-Co shells, we infer that indeed Co is present as a dispersed CoS_x phase. In line with the indications of redispersion seen in MES, the Co–Co coordination number decreases above a sulfidation temperature of 300 °C. The results are essentially the same after 0.1 MPa sulfidation at 400 °C. Similar to the findings from Mo K-edge EXAFS, only high-pressure sulfidation brings about sufficient order in the active phase that a Co–Mo interaction can be distinguished in the spectra. It is also noteworthy that the Co–S coordination number after sulfidation at 400 °C remains well below a value of 6, stressing further that full sulfidation has not occurred and the active phase has a significant type I character. Altogether, these structural data are very similar to what has been reported before for CoMo/γ-Al_2O_3 catalysts [28].

3.2. Catalytic performance

The gas-phase DBT HDS activities of Co(1.3)Mo(7)/C, Co(2.25)Mo(7)/C and Co(2.25)Mo(7)/Al_2O_3 sulfided at 0.1 and 4.0 MPa are given in Table 5. The pseudo first-order rate constants are determined from the DBT conversion after 8 h time on stream at 30 bar and 300 °C. As expected, the carbon-supported catalysts are much more active than the alumina-supported CoMo catalyst. It can be seen that the sulfidation pressure significantly influences the DBT HDS activities. Co(1.3)Mo(7)/C after sulfidation at 4.0 MPa is twice as active as the catalyst sulfided at 1 bar sulfidation. The

Table 2
MES parameters of Co(2.25)Mo(7)/C catalyst after different sulfidation treatments.

T_s (°C)	P (MPa)	IS (mm s^{-1})	QS (mm s^{-1})	Γ (mm s^{-1})	A (%)	IS (mm s^{-1})	QS (mm s^{-1})	Γ (mm s^{-1})	A (%)	IS (mm s^{-1})	QS (mm s^{-1})	Γ (mm s^{-1})	A (%)
		"Co-oxide"				"Co-sulfide"				"High-spin 2+"			
Fresh		0.29	0.73	0.66	58.7					0.88	1.74	0.59	41.3
RT	0.1					0.21	1.19	0.77	100				
100	0.1					0.18	1.22	0.72	100				
200	0.1					0.22	0.81	0.67	100				
300	0.1					0.23	0.85	0.73	100				
400	0.1					0.23	0.84	0.75	100				
						"Co–sulfide"				Co_9S_8			
400	4					0.21	0.98	0.66	63.1	0.25	0.29	0.46	36.9

Table 3
Mo K-edge EXAFS fit parameters for Co(1.3)Mo(7)/C catalyst after different sulfidation treatments.

Treatment	N (−)	R (Å)	$\Delta\sigma^2$ ($\cdot 10^{-3}$ Å^2)	ΔE_0 (eV)	N (−)	R (Å)	$\Delta\sigma^2$ ($\cdot 10^{-3}$ Å^2)	ΔE_0 (eV)	N (−)	R (Å)	$\Delta\sigma^2$ ($\cdot 10^{-3}$ Å^2)	ΔE_0 (Ev)
	Mo–S				Mo–Mo				Mo–Co			
S, 0.1 MPa, 200 °C	5.7	2.46	5.4	0.8	1.3	2.73	4.5	4.6				
S, 0.1 MPa, 300 °C	4.6	2.41	3.7	1.5	2.3	3.13	6.2	4.1				
S, 0.1 MPa, 400 °C	5.3	2.41	2.7	2.6	2.9	3.15	4.1	2.6				
S, 0.1 MPa + S, 4 MPa, 400 °C	5.7	2.42	2.1	2.5	3.6	3.15	4.1	4.6	0.5	2.75	8.6	9.8

Table 4
Co K-edge EXAFS fit parameters for Co(1.3)Mo(7)/C catalyst after different sulfidation treatments.

Treatment	Co–S				Co–Co (1)				Co–Mo				Co–Co (2)			
	N (–)	R (Å)	$\Delta\sigma^2$ ($\cdot 10^{-3}$ Å^2)	ΔE_0 (eV)	N (–)	R (Å)	$\Delta\sigma^2$ ($\cdot 10^{-3}$ Å^2)	ΔE_0 (eV)	N (–)	R (Å)	$\Delta\sigma^2$ ($\cdot 10^{-3}$ Å^2)	ΔE_0 (eV)	N (–)	R (Å)	$\Delta\sigma^2$ ($\cdot 10^{-3}$ Å^2)	ΔE_0 (eV)
S, 0.1 MPa, 200 °C	5.1	2.22	3.6	0.4	2.0	2.56	9.5	−3.4					1.2	3.29	9.9	9.5
S, 0.1 MPa, 300 °C	5.2	2.23	3.4	−0.8	1.3	2.57	5.8	−3.0					1.3	3.29	9.6	9.5
S, 0.1 MPa, 400 °C	5.3	2.23	3.6	−1.1	1.2	2.57	5.6	−2.2					1.2	3.29	9.7	9.5
S, 0.1 MPa + S, 4 MPa, 400 °C	5.6	2.23	4.2	−1.2	1.4	2.60	9.5	−1.4	1.1	2.80	9.6	−9.7	0.9	3.35	9.8	9.8

Table 5
Catalytic activities of CoMo/C catalysts in gas-phase DBT HDS.

Pretreatment	DBT HDS k ($mol_{DBT}\ kg_{Mo}^{-1}\ s^{-1}$)[a]
Co(1.3)Mo(7)/C	3.8×10^{-2}
S, 0.1 MPa, 400 °C	n.d.[b]
S, 4 MPa, 400 °C	6.0×10^{-2}
S, 0.1 MPa + S, 4 MPa, 400 °C	
Co(2.25)Mo(7)/C	3.0×10^{-2}
S, 0.1 MPa, 400 °C	10.1×10^{-2}
S, 4 MPa, 400 °C	8.1×10^{-2}
S, 0.1 MPa + S, 4 MPa, 400 °C	
Co(2.25)Mo(7)/Al_2O_3	1.5×10^{-2}
S, 0.1 MPa, 400 °C	3.1×10^{-2}
S, 4 MPa, 400 °C	

[a] First-order rate constant at 300 °C (200 ppm DBT).
[b] Not determined.

increase in DBT HDS activity for CoMo(2.25)Mo(7)/C upon high-pressure sulfidation is significantly larger than for Co(1.3)Mo(7)/C. The DBT HDS activity of Co(2.25)Mo(7)/C after 1 bar sulfidation is somewhat lower than for Co(1.3)Mo(7)/C. We tentatively attribute this to the relatively low CoS_x dispersion, which may result in partial blockage of the 'Co–Mo–S' phase. The more substantial activity increase following high-pressure sulfidation for Co(2.25)Mo(7)/C should be related to Co_9S_8 segregation and the concomitant better ordering of the 'Co–Mo–S' phase. The sample directly sulfided at 4.0 MPa is somewhat more active than the one after sequential sulfidation at 0.1 and 4.0 MPa. This small difference can be traced back to a slightly higher contribution of the 'Co–Mo–S' phase deduced from the MES data. This strong activity increase points to more pronounced type II phase character of the active 'Co–Mo–S' phase in agreement with the EXAFS data. As the Mo K-edge EXAFS data appear to indicate that the complete sulfidation also resulted in changes in the MoS_2 dispersion, we evaluated the performance of Co(2.25)Mo(7)/C in thiophene HDS (sulfidation at 400 °C, reaction at 350 °C, 4 vol% thiophene in H_2). Co(2.25)Mo(7)/C sulfided at 0.1 MPa was about twice as active in thiophene HDS as the same catalyst sulfided at 4.0 MPa (86 $mol_{thiophene}\ mol_{Mo}^{-1}\ h^{-1}$ vs. 39 $mol_{thiophene}\ mol_{Mo}^{-1}\ h^{-1}$). This difference is remarkable in view of the opposite activity order in DBT HDS. Perhaps the most reasonable explanation may be as follows. After 0.1 MPa sulfidation the active phase is highly dispersed (low Mo–Mo coordination number, Table 3; cf. ref. [37]), in relatively strong interaction with the support (low Mo–S coordination number), and partially blocked in the micropores of the carbon support, where it is accessible to thiophene, but not to DBT molecules. An increase of the sulfidation pressure leads to more of a type II Co–Mo–S phase, but also to some sintering, sufficient to have the active phase migrate to larger pores where it becomes also accessible to DBT. In this picture, then, thiophene HDS decreases because of the decrease of active-phase dispersion, while DBT HDS strongly increases because of the increased formation of type-II Co–Mo–S on the one hand, and the increased accessibility of the active phase compensating for the loss of dispersion on the other. But in any case, as pointed out above, independent of the sulfidation pressure, the CoMo/C catalysts are more active in DBT HDS than their alumina-supported counterparts (Table 5). Such a large difference has been reported before [39,40] and has been argued to originate from a more favourable interaction of the 'Co–Mo–S' species with the carbon support [41] (cf. Section 3.1 above).

Although the difference in structural effects between 0.1 and 4.0 MPa sulfidation is not completely clear, it is evident that the MoS_2 dispersion in CoMo/C after 4.0 MPa sulfidation remains good and that the gas-phase DBT HDS activity of CoMo/C is higher than that of CoMo/Al_2O_3. Therefore, our further work focused on the

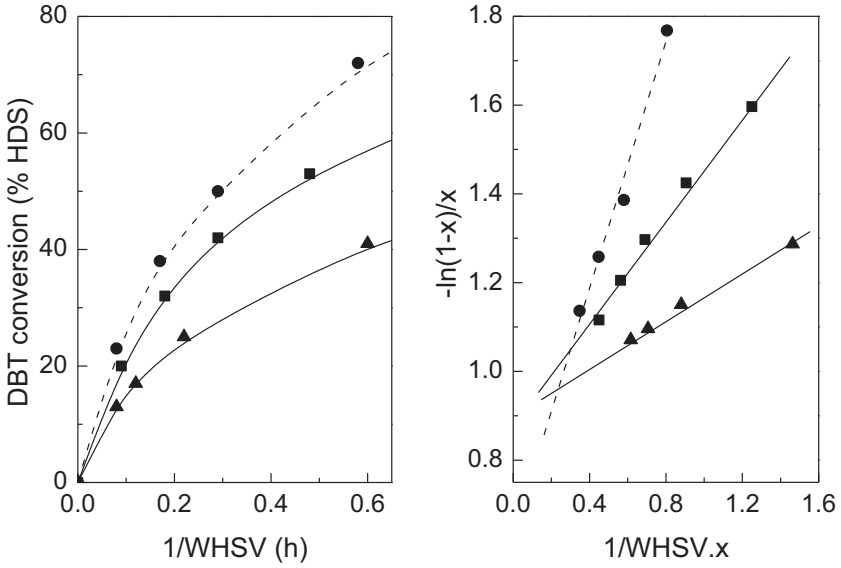

Fig. 2. (left) DBT HDS conversion (trickle flow, 3.5 MPa, 340 °C, 250 Nl_{H_2} kg^{-1}_{feed}, 4.8 wt% DBT in *n*-hexadecane) and (right) kinetic plot according to Eq. (1) for (●) NiMo-NTA/C, (■) commercial NiMo/γ-Al_2O_3 and (▲) NiMo-NTA/γ-Al_2O_3.

suitability of a carbon-supported M′Mo catalyst (we employed the NiMo composition in this part) in test reactions more close to industrial hydrotreating operations. As reference catalysts, we employed a NiMo-NTA/γ-Al_2O_3 catalyst and an older-generation commercial NiMoP/γ-Al_2O_3 catalyst (predominantly a type I 'Ni–Mo–S' phase, cf. ref. [31]). The NiMo-NTA/C catalysts had twice the thiophene HDS activity of its γ-Al_2O_3-supported analogue as reported before [12]. The DBT HDS activities of these catalysts are compared in Fig. 2a. It appears that under trickle-flow conditions (i) NiMo-NTA/C is much more active than its γ-Al_2O_3 analogue, i.e., as in the case of thiophene HDS (and gas-phase DBT HDS for similar CoMo catalysts) there is a clear support effect on the HDS performance of type II 'Ni–Mo–S', and (ii) the carbon support in fact increases the type II 'Ni–Mo–S' activity to a level above that of a commercial, although outdated, NiMo catalyst. The kinetics of DBT HDS for the three catalysts are compared in Fig. 2b. The model equation employed here is a linearization of a Langmuir-Hinshelwood model for the DBT HDS reaction (see for instance Broderick and Gates [42]) involving separate sites for adsorption of DBT, possible intermediates and the products, and for H_2

$$\frac{\ln(1-x)}{1} = \frac{kK_{H_2}p_{H_2}}{1+K_{H_2}p_{H_2}} \cdot \frac{K_{DBT}}{K_{products}} \cdot \frac{1}{WHSV \cdot x} + \left(1 - \frac{K_{DBT}}{K_{products}}\right) \quad (1)$$

with x being the DBT conversion, k the rate constant, K_i the adsorption constant of compound i and *WHSV* the weight hourly space velocity. Fig. 2b shows that the DBT HDS kinetics of NiMo–NTA/C are quite different from those of the alumina-supported analogues, in that the $(1\text{-}K_{DBT}/K_{products})$ term appears to be much lower. The HDS products are essentially H_2S and biphenyl. Disregarding the latter for the moment, since normally $K_{H2S} \gg K_{biphenyl}$ on sulfided catalysts and observing that addition of H_2S to NiMo-NTA/C had effects comparable to those usually encountered, we conclude that apparently DBT is much more able to compete with H_2S for the 'Ni–Mo–S' adsorption sites in carbon-supported than in the oxide-supported catalyst systems.

The activity of NiMo-NTA/C for the HDN of quinoline, that is, its conversion into hydrocarbons and ammonia, is compared with that of NiMo-NTA/γ-Al_2O_3 in Fig. 3. In the case of the alumina-supported catalyst, the reaction order in quinoline is zero at 308 °C and slightly positive at 330 °C, whereas in the case of NiMo-NTA/C it is negative. The best fit for the activity curves of the carbon-supported catalyst determined at 290 and 308 °C gives a reaction order in quinoline of −0.4. These negative reaction orders are a consequence of quinoline strongly adsorbing on the catalyst surface. As a consequence, lowering the N content of the feed would increase the activity advantage of the carbon-supported catalyst even further. Thus, it can be concluded that type II 'Ni–Mo–S' on activated carbon is significantly more active in single component HDS and HDN test reactions than its alumina counterpart.

It was therefore decided to evaluate the performance of NiMo-NTA/C in hydrotreating a real feed, in this case a catalytically cracked heavy gas oil. Recently, Maity et al. reported about the influence of the support on the heavy oil hydrotreating activity of CoMo

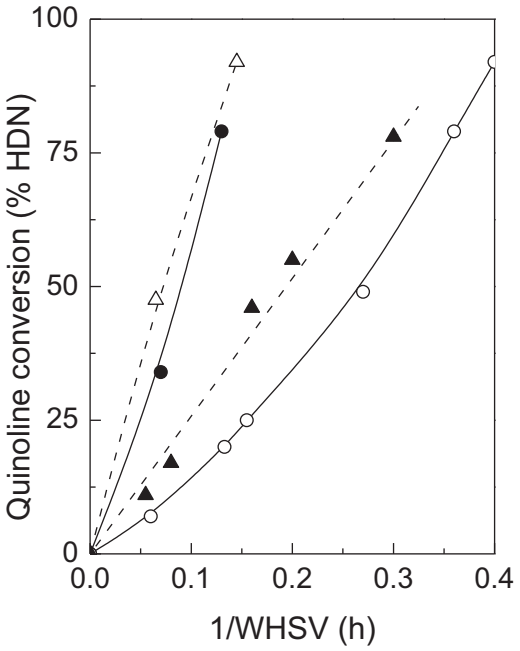

Fig. 3. Quinoline HDN conversion (trickle flow, 6 MPa, 340 °C, 250 Nl_{H_2} kg^{-1}_{feed}, 1560 ppmw N as quinoline in *n*-hexadecane) for (●,○) NiMo-NTA/C and (▲,△) NiMo-NTA/γ-Al_2O_3 at (△) 330 °C, (●,▲) 308 °C and (○) 290 °C.

sulfide catalysts [43]. These authors found that a CoMo sulfide supported on an activated carbon carrier, which performed quite well in thiophene HDS, quickly lost its HDS and HDM (hydrodemetallization) activity when used to hydrotreat a heavy oil. In that particular case, however, we believe that deactivation was mostly induced by pore plugging of the support by precipitation of metal sulfides from the oil, which is related to the specific texture of the support [44]. In our case, the CCHGO feed does not contain significant amounts of metals. It turns out that the performance in hydrotreating of a CCHGO feed of our NiMo-NTA/C catalyst was substantially lower than that of the commercial NiMoP/γ-Al_2O_3. In percentages of the commercial catalyst, NiMo-NTA/C had a HDN activity of 41%, a HDS activity of 75% and for hydrogenation 95%. As typically the DBT HDS and quinoline HDN tests do appear to reflect the real-feed performance of alumina-supported catalysts rather well, an effort was made to understand the possible cause of the NiMo-NTA/C failure. From the kinetics, it emerged that reactant adsorption effects play a much larger role for the carbon-supported catalyst than for the alumina-supported ones. The negative order in quinoline indicates that adsorption of (hydrogenated) quinoline inhibits the activation of hydrogen, while in the case of the alumina counterpart the reaction order never dropped below zero. For DBT, stronger competition for the adsorption sites on the carbon-supported catalysts is noted. Thus, there is the distinct possibility that also polycyclic aromatics, another class of strongly adsorbing species, stick more firmly onto sulfided NiMo-NTA/C than onto sulfided alumina-supported NiMo. Taking into account that the CCHGO feed contained more than 50% aromatics, mostly bi- and tri-cyclics, we therefore hypothesized that strong adsorption of (poly)aromatic molecules is causing the bad performance of the NiMo-NTA/C in the CCHGO test. This hypothesis was checked as follows. A feed was prepared containing 0.6 wt% S as DBT, 880 ppw N as quinoline in *n*-hexadecane (the CCHGO feed contains 2.59 wt% S and 900 ppmw N). At a H_2 pressure of 6.0 MPa and a temperature of 290 °C and WGS = 6 h^{-1} HDS was complete over the NiMo-NTA/C catalyst, as expected. After stabilization, the HDN conversion amounted to 48% (HDN conversion in the absence of DBT was 65%). Without changing the operating conditions, 3 wt% phenanthrene was added to the feed. This resulted in a decrease of the HDN conversion to 36%. At this level, no effect at all is to be expected for a NiMo/Al_2O_3 catalyst [45]. Thus, the outcome of this experiment is in accordance with our hypothesis.

These trickle-flow hydrotreating tests inform us that the performance of NiMo/C in the hydrotreatment of a catalytically cracked heavy gas oil is much poorer than anticipated on the basis of HDS and HDN model experiments. The reason appears to be that, while the intrinsic activity of NiMo/C is very high, polyaromatic molecules adsorb much stronger on the active NiMo sulfide phase when it is supported on carbon than when it is supported on alumina, with the concomitant reduction of the catalyst performance. This conclusion is in agreement with the findings of Saito et al. [25], who report that in the case of a *light* gasoil, where the polyaromatics concentration will be low, carbon-supported NiMo remains better than its alumina-supported counterpart. On the other hand, the feed used by Adjaya et al. appears to be fully as nasty as ours, and they still conclude that their NiMo/mesoporous carbon performs better than NiMo/Al_2O_3, at least on a weight basis. As the nitrogen content of their feed is rather high, we surmise that the N-bearing molecules may compete more effectively for the adsorption sites than in our case. While, therefore, M′Mo/C formulations may have a chance in some niche applications, in general, taking also into account the well-known drawbacks of the use of carbon, namely that its density is rather low (about 30% less than that of an equivalent Al_2O_3-supported catalyst), low mechanical strength and that its regenerability is questionable, the corollary of all this is that carbon will most likely not find any extensive application as a carrier material for industrial hydrotreating catalysts.

4. Conclusions

From the present study of the sulfidation of CoMo/active carbon with ^{57}Co MES and EXAFS, and of the performance of its NiMo counterpart in various hydrotreating reactions, the following conclusions can be drawn:

1. Sulfidation at 0.1 MPa H_2/H_2S of Co(1.3)Mo(7)/C leads to the formation of a highly dispersed Co–Mo–S phase with pronounced type I character (low Mo–S coordination number, specifically). Its Co(2.25) counterpart has more Co than the edges of the MoS_2 can accommodate in atomic form, and CoS_x clusters are formed there.
2. Sulfidation at 4 MPa H_2/H_2S of Co(1.3)Mo(7)/C leads to the formation of a slightly less dispersed Co–Mo–S phase of a more type II character. In its Co(2.25) counterpart the higher pressure leads to a phase separation, into Co_9S_8 and Co–Mo–S.
3. These structural data are very similar to those reported before for CoMo/alumina [28], with this difference that the type I → type II conversion at higher pressure appears to be accompanied by some sintering of the MoS_2 particles. This could imply that the interaction between the active phase and the support is indeed weaker for C than for Al_2O_3 as one would tend to expect, although strong enough to prevent the full formation of Co–Mo–S type II even at the higher pressure.
4. The gas-phase DBT and thiophene HDS activities do not run parallel as the pressure increases: the former is enhanced, while the latter is decreased. We rationalize this in terms of the micropores of the active carbon occluding the MoS_2 particles to some extent, such that they can be reached by thiophene, but not by DBT molecules. Elucidation of this aspect would necessitate further work.
5. In the liquid-phase HDS of DBT and HDN of quinoline (trickle-flow-presulfidation at 4 MPa) NiMo/C outshines NiMo(P)/alumina, as indeed it does for gas-phase DBT HDS. The kinetics show that DBT adsorption on the active sites is much more competitive with H_2S for the former as compared with the latter, and that quinoline is so strongly adsorbed that its reaction order becomes negative.
6. In the Cat-cracked heavy gasoil test, however, NiMo/C loses out to its alumina counterpart, and this is probably due to the competitive adsorption of poly-aromatics. Adding 3%wt phenanthrene to the model DBT + quinoline feed (under conditions where HDS was 100%, and the HDN around 50%) did indeed lead to a sizable loss of HDN activity.

Acknowledgements

The authors wish to acknowledge Mr. H.A. Colijn and Mr. A. F. de Vries of the Shell laboratory, Amsterdam, for their help with the trickle-flow tests and Mr. A.E. Coumans of Eindhoven University of Technology for carrying out the thiophene HDS tests.

References

[1] R. Prins, V.H.J. de Beer, G.A. Somorjai, Catalysis Reviews: Science and Engineering 31 (1989) 1.
[2] H. Topsøe, B.S. Clausen, F.E. Massoth, Hydrotreating catalysis, Springer, Berlin, 1996.
[3] P.T. Vasudevan, J.L.G. Fierro, Catalysis Reviews: Science and Engineering 38 (1996) 161.
[4] S. Eijsbouts, Applied Catalysis A 158 (1997) 53.
[5] M. Breysse, E. Furimsky, S. Kasztelan, M. Lacroix, G. Perot, Catalysis Reviews 44 (2002) 651.
[6] H. Topsøe, B.S. Clausen, R. Candia, C. Wivel, S. Mørup, Journal of Catalysis 68 (1981) 433.
[7] C. Wivel, R. Candia, B.S. Clausen, S. Mørup, H. Topsøe, Journal of Catalysis 68 (1981) 453.

[8] J.A.R. van Veen, E. Gerkema, A.M. van der Kraan, P.A.J.M. Hendriks, H. Beens, Journal of Catalysis 133 (1992) 112.
[9] M.W.J. Crajé, V.H.J. de Beer, A.M. van der Kraan, Hyperfine Interaction 69 (1991) 795.
[10] M.W.J. Crajé, V.H.J. de Beer, J.A.R. van Veen, A.M. van der Kraan, Applied Catalysis A 100 (1993) 97.
[11] M. Breysse, P. Afanasiev, C. Geantet, M. Vrinat, Catalysis Today 86 (2003) 5.
[12] J.A.R. van Veen, E. Gerkema, A.M. van der Kraan, A. Knoester, Journal of the Chemical Society, Chemical Communication (1987) 1684.
[13] R. Candia, O. Sorensen, J. Villadsen, N.-Y. Topsøe, B.S. Clausen, H. Topsøe, Bulletin des Societes Chimiques Belges 93 (1984) 763.
[14] J.P.R. Vissers, V.H.J. de Beer, R. Prins, J. Chem Soc, Faraday Transactions 1 83 (1987) 2145.
[15] L. Kaluza, D. Gulkova, Z. Vit, M. Zdrazil, Applied Catalysis A 324 (2007) 30.
[16] M. Hussain, J.S. Yun, S.-K. Ihm, N. Russo, F. Geobaldo, Industrial and Engineering Chemistry Research 50 (2011) 2530.
[17] H. Topsøe, R. Candia, N.-Y. Topsøe, B.S. Clausen, Bulletin des Societes Chimiques Belges 93 (1984) 783.
[18] W.R.A.M. Robinson, J.A.R. van Veen, V.H.J. de Beer, R.A. van Santen, Fuel Processing Technology 61 (1999) 89.
[19] V.H.J. de Beer, J.C. Duchet, R. Prins, Journal of Catalysis 72 (1981) 369.
[20] J.C. Duchet, E.M. van Oers, V.H.J. de Beer, R. Prins, Journal of Catalysis 80 (1983) 386.
[21] M.W.J. Crajé, V.H.J. de Beer, A.M. van der Kraan, Applied Catalysis 70 (1991) L7.
[22] M.W.J. Crajé, S.P.A. Louwers, V.H.J. de Beer, R. Prins, A.M. van der Kraan, Journal of Physical Chemistry 96 (1992) 5445.
[23] S.M.A.M. Bouwens, J.A.R. van Veen, D.C. Koningsberger, V.H.J. de Beer, R. Prins, Journal of Physical Chemistry 95 (1991) 123.
[24] A.I. Dugulan, M.W.J. Crajé, A.R. Overweg, G.J. Kearley, Journal of Catalysis 229 (2005) 276.
[25] M. Kouzu, Y. Kuriki, F. Hamdy, K. Sakanishi, Y. Sugimoto, I. Saito, Applied Catalysis 265 (2004) 61.
[26] N. Prabhu, A.K. Dalai, J. Adjaya, Applied Catalysis A 401 (2011) 1.
[27] A.I. Dugulan, M.W.J. Crajé, G.J. Kearley, Journal of Catalysis 222 (2004) 281.
[28] A.I. Dugulan, E.J.M. Hensen, J.A.R. van Veen, Catalysis Today 130 (2008) 126.
[29] H.R. Reinhoudt, C.H.M. Boons, A.D. van Langeveld, J.A.R. van Veen, S.T. Sie, J.A. Moulijn, Applied Catalysis A 207 (2001) 25.
[30] M.W.J. Crajé, PhD Thesis, Delft University of Technology, Delft, 1992, ISBN 90-73861-08-X.
[31] A.I. Dugulan, PhD Thesis, Delft University, The Netherlands, 2008, ISBN 978-1-58603-863-2.
[32] J.G. Steven, L. Zhe, H. Pollak, V.E. Stevens, R.H. White, J.L. Gibson, Mössbauer Handbook Minerals, Mössbauer Effect Data Center, University of North Carolina, Asheville, 1983.
[33] E.J.M. Hensen, Y. van der Meer, J.A.R. van Veen, J.W. Niemantsverdriet, Applied Catalysis A 322 (2007) 16.
[34] T.G. Parham, R.P. Merrill, Journal of Catalysis 85 (1984) 295.
[35] M. de Boer, A.J. van Dillen, D.C. Koningsberger, J.W. Geus, Japanese Journal of Applied Physics 32 (1992) 460.
[36] R. Cattaneo, T. Weber, T. Shido, R. Prins, Journal of Catalysis 191 (2000) 225.
[37] S.M.A.M. Bouwens, F.B.M. van Zon, M.P. van Dijk, A.M. van der Kraan, V.H.J. de Beer, J.A.R. van Veen, D.C. Koningsberger, Journal of Catalysis 146 (1994) 375.
[38] S.M.A.M. Bouwens, D.C. Koningsberger, V.H.J. de Beer, S.P.A. Louwers, R. Prins, Catalysis Letters 5 (1990) 273.
[39] E.J.M. Hensen, V.H.J. de Beer, J.A.R. van Veen, R.A. van Santen, Journal of Catalysis 215 (2003) 353.
[40] H. Farag, I. Mochida, K. Sakanishi, Applied Catalysis A 194/195 (2000) 147.
[41] H. Farag, D. Whitehurst, I. Mochida, Industrial and Engineering Chemistry Research 37 (1998) 3533.
[42] D.H. Broderick, B.C. Gates, AIChE Journal 27 (1981) 663.
[43] S.K. Maity, E. Blanco, J. Ancheyta, F. Alonso, H. Fukuyama, Fuel 100 (2012) 17.
[44] J.M. Oelderik, S.T. Sie, D. Bode, Applied Catalysis 47 (1989) 1.
[45] A.J. van Welsenes, J.A.R. van Veen, unpublished data;
N.K. Nag, Applied Catalysis 10 (1984) 53.